

The effect of albite additions on the sintering, phase compositions and microstructure of vitreous ceramic tiles

N.M. Khalil^{a, b}, M.M.S. Wahsh^b and Amany Gaber^b

^aDepartment of Chemistry, Faculty of Sciences and Arts, Khulais, University of Jeddah, Saudi Arabia

^bRefractories, Ceramics and Building Materials Dept., National Research Centre, 12311 Cairo, Egypt

Vitreous ceramic tiles were produced from clay, quartz and albite mixtures fired at 1150 °C. These ceramic tiles were classified according to the ISO standard. The effect of fluxes additions on the technological properties of ceramic tiles has been studied. The sintering behavior (linear shrinkage, water absorption, apparent porosity and bulk density) of the prepared ceramic bodies was followed. Phase compositions and microstructure were characterized by X-ray diffraction (XRD) and scanning electron microscope (SEM) attached with an EDAX unit. The densification parameters and hence mechanical properties of the samples were enhanced with increasing of albite content up to 40 wt. % due to liquid phase sintering mechanism. However, higher amount of fluxes above the vitrification range (> 40 wt.%) results in a noticeable decrease in the sintering and mechanical properties.

Key words: Vitreous ceramic tiles, Water absorption, X-ray diffraction, Microstructure.

Introduction

The world consumption of ceramic products has steadily increased during the last few years to satisfy their urgent need associated with the boom in the field of construction activity [1]. Kaolin, quartz and feldspar are mainly the raw materials used for different types of ceramic products industry. This industry is one of the main industries in countries containing huge reserves of such raw materials [2, 3]. The worldwide production of ceramic tiles reaches about 8500 million square meters which makes them as one of the most commonly consumed material [3]. Such an impressive growth implies an increasing demand for raw materials. So several research works have been carried on using different raw materials for ceramics industry [4, 5]. Vitreous ceramic bodies are commonly manufactured from blends consisting of alumina-rich clay minerals (plastic materials), quartz (filler) and feldspars, which are natural fluxing agents [6, 7]. Phase diagram illustrating the standard composition of vitreous ceramic is shown in Fig. 1 [8]. Kaolinitic clay plays an essential role during ceramic industry either in the green or in the fired state. It assists plasticity of the green paste which facilitates the shaping process, after firing it promotes mullite formation which improves the physicommechanical properties of the prepared ceramic bodies. Quartz is necessary as filler maintaining the volume stability of the fired bodies. Feldspar acts as a fluxing agent enhances glassy phase

formation which promotes the mullite crystal growth and hence improves the sintering process through filling interconnected pores. Such fluxes give rise to a viscous liquid phase, which plays a key role in the consolidation of ceramic bodies [9]. Because of their low water absorption and good mechanical resistance [7, 10], vitreous ceramic bodies are extensively used as table wares, sanitary objects, floor and wall tiles, and have been the subject of numerous studies [11-18]. Vitreous tiles are widely used as colorful aesthetically-pleasing mosaics as well as wall coverings in bathrooms, kitchens and living rooms. Chemical and mineralogical compositions of the raw materials as well as the firing conditions (temperature, time, rate and atmosphere) are the main factors controlling the technological properties of the ceramic bodies [11, 12, 19, 20]. Given the numerous possible combinations between the latter

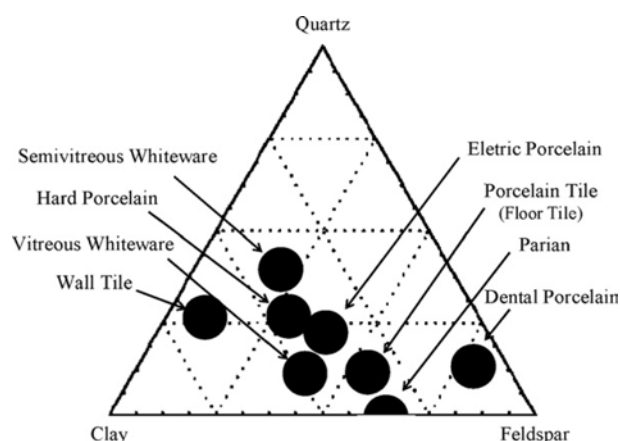


Fig. 1. Phase diagram of triaxial ceramic products [8].

*Corresponding author:
Tel : +00966548959278
E-mail: nagy2071@yahoo.com

parameters, their manufacturing requires many trials. Thereby, in this study, utilization of two new fluxes and the effects of their content on some technological properties including water absorption, linear firing shrinkage, cold crushing strength, phase composition and microstructure have been studied to obtain high performance vitreous ceramic products.

Materials and Experimental Details

Materials

The starting raw materials used for the preparation of ceramic bodies are Egyptian clay and quartz in addition to two sources of Saudian albite (one from Gholaa and the other from Osfan, West of KSA). Their chemical analysis was determined using XRF technique.

Preparation and investigation of ceramic bodies

Two series of the ceramic tile batches were prepared using two different albite raw minerals as fluxes. The individual batches were well mixed in a ball mill for 2 h and then shaped into cylindrical bodies through uniaxially semi-dry pressed at 150 MPa. The obtained green bodies were dried overnight at 110 °C and fired at 1150 °C with the firing rate 10 °C/min and a soaking time of 2 h. Solid phase compositions of the fired samples were estimated by X-ray diffraction (XRD instrumental D8 advance, Bruker, Germany; monochromatic beam with $K\alpha_1$ Cu, Bragg Brentano geometry θ . 2 θ and linear detector LYNX EYE 174 channels 2 s/channel, total time = 348 s. The morphology and microchemistry of the fired bodies were investigated using scanning electron microscope (SEM; Philips XL 30) attached with an EDX unit.

Characterization of the prepared ceramic bodies

The densification parameters in terms of bulk density, apparent porosity and water absorption were determined used kerosene displacement technique based on Archimedes assumption according to ISO 10545-3:1995. The linear change of ceramic materials measures their volume shrinkage after firing according to ASTM C531; it is tested and calculated from the next equation:

Cold crushing strength (CCS) was measured according to ASTM: C133-97 using a hydraulic press machine (SEIDNR-Riedlinger, Germany). It is defined as capability of the sample to resist vertical stress; $CCS = \text{stress/area}$, the area here is the surface area of the cylindrical bodies (area of the circle, πr^2). This test tells us how much load that ceramic material can bear in cold conditions.

Results and Discussion

The chemical analysis of the starting raw materials is presented in Table 1. The main constituents of the clay

Table 1. Chemical analysis of the starting raw materials.

Oxides	Clay	Gholaa albite	Osfan albite
Na ₂ O	0.16	4.328	4.015
MgO	0.20	4.864	8.55
Al ₂ O ₃	27.29	14.009	17.008
SiO ₂	59.50	47.08	51.082
P ₂ O ₅	---	0.379	0.456
SO ₃	---	0.100	0.099
K ₂ O	1.28	0.540	1.879
CaO	0.22	4.183	1.400
TiO ₂	1.96	1.454	1.394
Cr ₂ O ₃	---	---	0.016
MnO	0.03	0.674	0.335
Fe ₂ O ₃	1.00	17.813	10.406
Co ₃ O ₄	---	0.033	0.024
NiO	---	0.029	0.013
ZnO	---	0.069	0.033
SrO	---	0.028	0.023
ZrO ₂	---	0.039	0.071
BaO	---	0.023	0.047
F	---	0.380	0.204
Cl	---	0.174	0.045
L.O.I.	8.200	3.800	2.900

are SiO₂ (59.50%) and Al₂O₃ (27.29%) in addition to minor amounts of Fe₂O₃ and alkalis (K₂O + Na₂O). Albite consists of 47-51% of SiO₂ and 14-17% of Al₂O₃ with some impurities, such as Fe₂O₃, CaO, MgO and TiO₂. High pure quartz (98% of SiO₂) was also used in this work.

Densification parameters

Fig. 2, Fig. 3 show the bulk density and apparent porosity behavior of the fired (1150 °C) ceramic bodies. From sample 1 to 3 and from sample 5 to 7 an increase in bulk density corresponded with a decrease in apparent porosity of the ceramic bodies is observed. This is correlated with the increase in the content of albite mineral which results in an increase in the content of liquid phase that fill the pores and cavities in the matrix resulting in an improved texture of the fired samples [21]. The fine pores create surface energy forces in the matrix of the ceramic body which allow the liquid phase to approach the particles leading to a

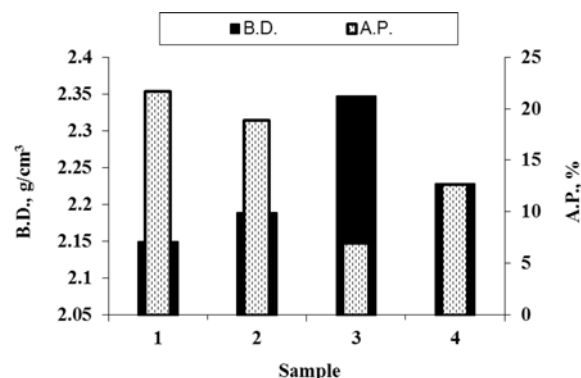


Fig. 2. Bulk density and apparent porosity of the samples 1-4 fired at 1150 °C.

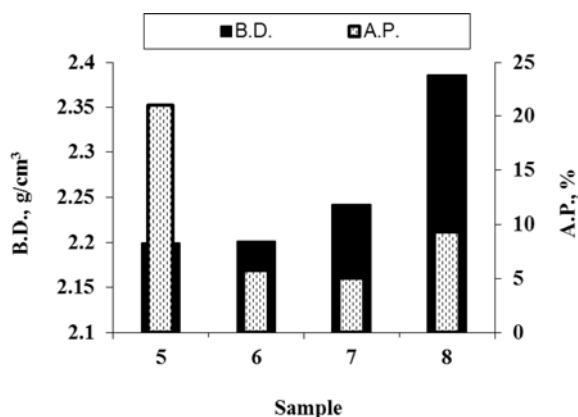


Fig. 3. Bulk density and apparent porosity of the samples 5-8 fired at 1150 °C.

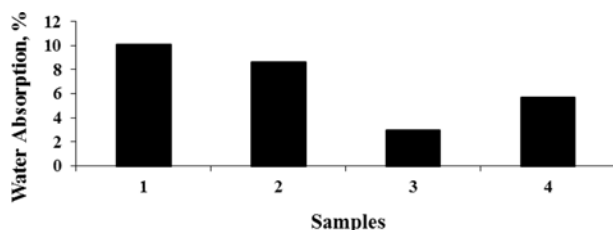


Fig. 4. Water absorption of the samples 1-4 fired at 1150 °C.

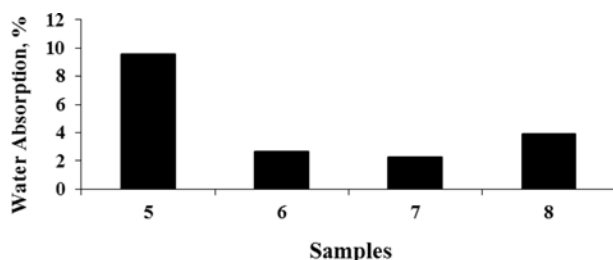


Fig. 5. Water absorption of the samples 5-8 fired at 1150 °C.

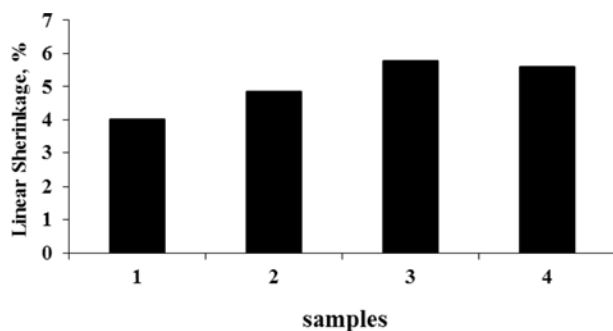


Fig. 6. Linear shrinkage of the samples 1-4 fired at 1150 °C.

decrease in the open porosity [17]. The water absorption behavior goes parallel to the apparent porosity i.e. it decreases with the decrease in the apparent porosity of the samples Figs. 4-5. However, samples 4 and 8 show an increase in the apparent porosity with increasing of albite content due to the increase of the liquid phase amount more than the optimum percent as well as the decrease of mullite phase with decreasing of clay content. According to the

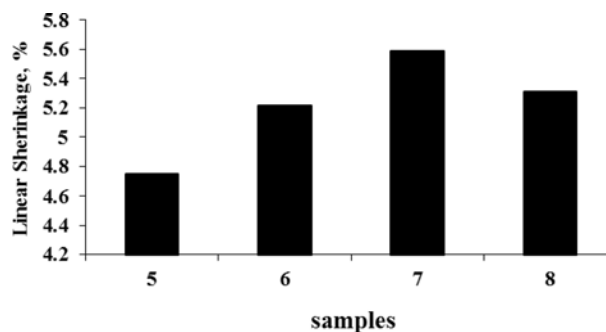


Fig. 7. Linear shrinkage of the samples 5-8 fired at 1150 °C.

ISO 13006 standard, ceramic samples 3 and 7 can be classified as group I (water absorption < 3%) and also sub-classified as group BIb (vitrified ceramic tiles, 0.5 % < water absorption < 3%). Figs. 6-7 show the linear shrinkage of the fired samples. The linear shrinkage was increased from sample 1-3 and 5-7 due to liquid phase sintering mechanism. Kingery [19, 22] proposed that the sintering process involving two stages. In the first the open porosity is decreased as a result of the fired sample shrinkage. In the second the constituents of the ceramic body make as a conjunction for small and closed pores. The ceramic body is densified as a result of surface energy forces inside the pores.

Cold crushing strength

As shown in Figs. 8-9, samples 3 and 7 show the highest cold crushing strength values in comparison with other samples due their relatively lower apparent porosity percent. The results show that increasing

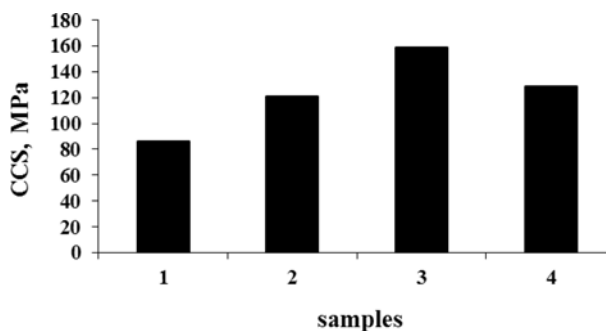


Fig. 8. Cold crushing strength of the samples 1-4 fired at 1150 °C.

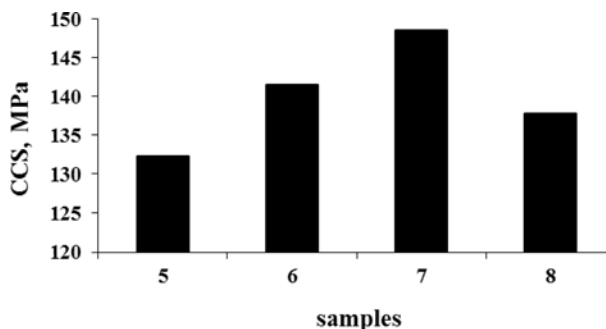


Fig. 9. Cold crushing strength of the samples 5-8 fired at 1150 °C.

porosity adversely affects the mechanical properties [21]. The strength of the ceramic body is related to felt-like interlocking of fine mullite needles, i.e. the strength of the ceramic body increases as the content of mullite increases [8, 19, 23]. The mismatch in the thermal expansion coefficient, between quartz particles [$\alpha \approx 15-26 \cdot 10^{-6} \text{ }^{\circ}\text{C}^{-1}$] and the silicate glass matrix [$\alpha \approx 5-8 \cdot 10^{-6} \text{ }^{\circ}\text{C}^{-1}$] generate a tensile hoop stress on the matrix, which leads to strength reinforcement in the ceramic bodies [21, 23]. According to this theory, a higher residual quartz content results in higher strength. So, the strength of the ceramic bodies is related to their porosity percent as well as mullite and quartz contents. The optimum vetrification range is achieved with minimum percent of apparent porosity and maximum linear shrinkage. Increasing in the content of liquid phase more than the vetrification range affects adversely the physical properties of the ceramic bodies.

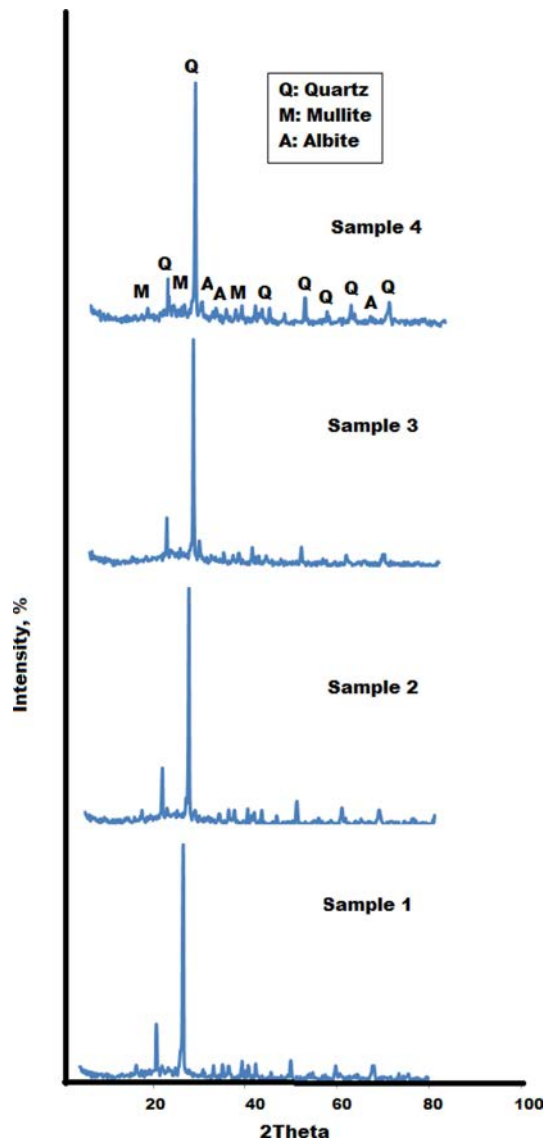


Fig. 10. XRD patterns of the samples 1-4 fired at 1150 °C.

In fact, the strength of the ceramic tiles is related to the variation in these all factors (porosity percent, mullite and quartz content). The optimum vetrification

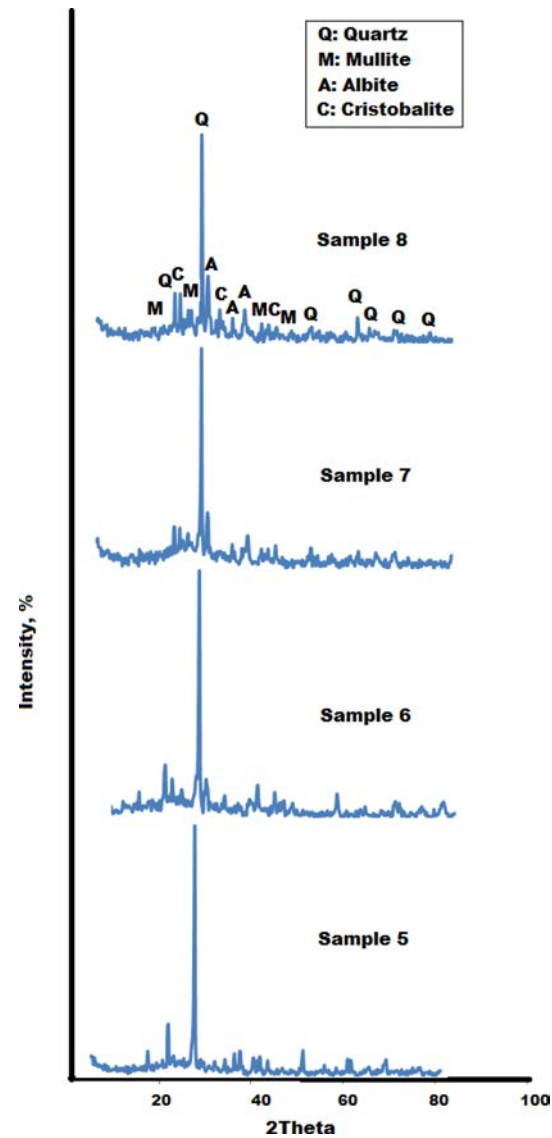


Fig. 11. XRD patterns of the samples 5-8 fired at 1150 °C.

Table 2. Compositions of the prepared mixes.

Sample	Mix composition, wt. %		
	Mixes containing Gholaa albite sample		
	Clay	Albite	Quartz
1	70	20	10
2	60	30	10
3	50	40	10
4	40	50	10
Sample	Mixes containing Osfan albite sample		
	Clay	Albite	Quartz
	Clay	Albite	Quartz
5	70	20	10
6	60	30	10
7	50	40	10
8	40	50	10

range is achieved in mixes 3 and 7 (mixes containing 40 wt. % albite) for which the linear change is maximum and the apparent porosity is in its minimum value. However, the increasing of liquid phase more than the vitrification range in mixes 4 and 8 results in a pronounced decrease in sintering and mechanical properties.

Solid phase composition

X-ray diffraction patterns shown in Fig. 10, Fig. 11 and their data given in table 3 indicate the solid phase compositions and their relative mass fractions of the fired ceramic samples. It is shown that the main phases are quartz (JCPDS card no. 5-490), mullite (JCPDS card no. 15-776) and albite (JCPDS card 9-0466) in addition to weak diffraction peaks of beta cristobalite (JCPDS Cards, No. 39-1425) (sample 8). Albite was disappeared in samples 1 and 4. However, the content of albite increases from sample 2 up to 4 and from sample 6 up to 8 with increasing of albite raw material addition. Mullite is decreased with decreasing of clay content. Mullite formed on firing is very dependent on the percentage of clay addition.

Microstructure

Figs. 12-13 show the microstructure and EDAX

Table 3. Phase compositions of the ceramic samples according to XRD data.

Sample	Mineral content. %			
	Ceramic bodies containing Gholaa albite sample			
	Quartz	Mullite	Albite	Cristobalite-beta
1	63.2	36.8	0	0
2	46.1	34.4	19.5	0
3	52.5	33.1	14.4	0
4	54	22.3	23.7	0
Sample	Ceramic bodies containing Osfan albite sample			
	Quartz	Mullite	Albite	Cristobalite-beta
	Quartz	Mullite	Albite	Cristobalite-beta
5	53.5	46.5	0	0
6	33.2	43.6	23.2	0
7	33.9	34.3	31.8	0
8	32.6	24.6	36.5	6.3

analysis of the selected samples 3 and 7 after firing at 1150 °C for 2 hrs. In sample 3, quartz and mullite were observed dispersed in the glassy phase. Quartz (point A) is present as large grains in the matrix surrounded by albite and mullite phases (Point B). However, in sample 7 quartz grains were partially dissolved in the

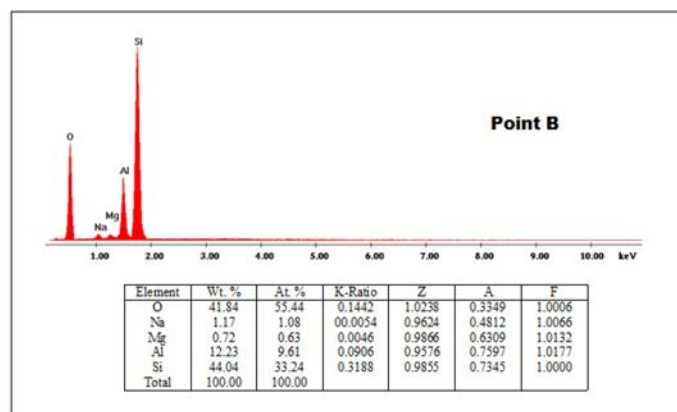
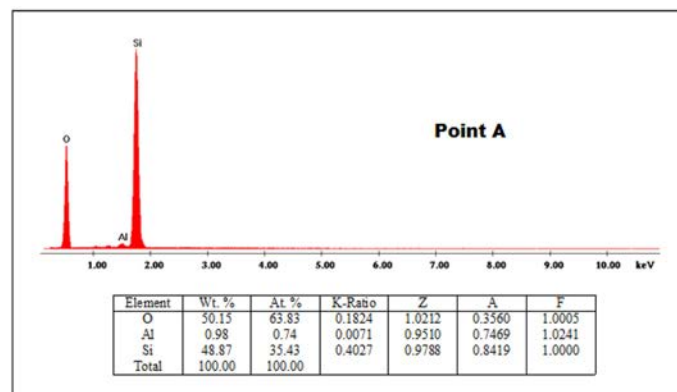
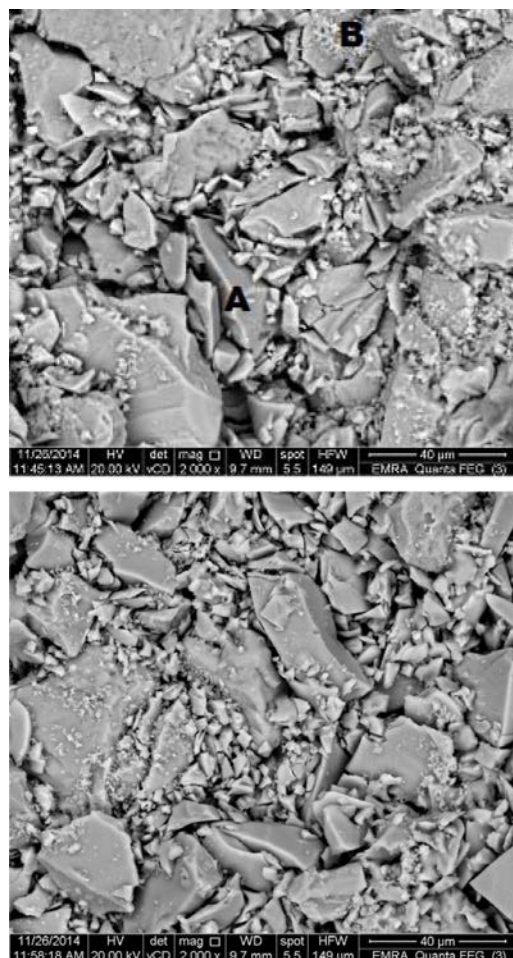


Fig. 12. SEM and EDAX analysis of the selected sample 3 fired at 1150 °C.

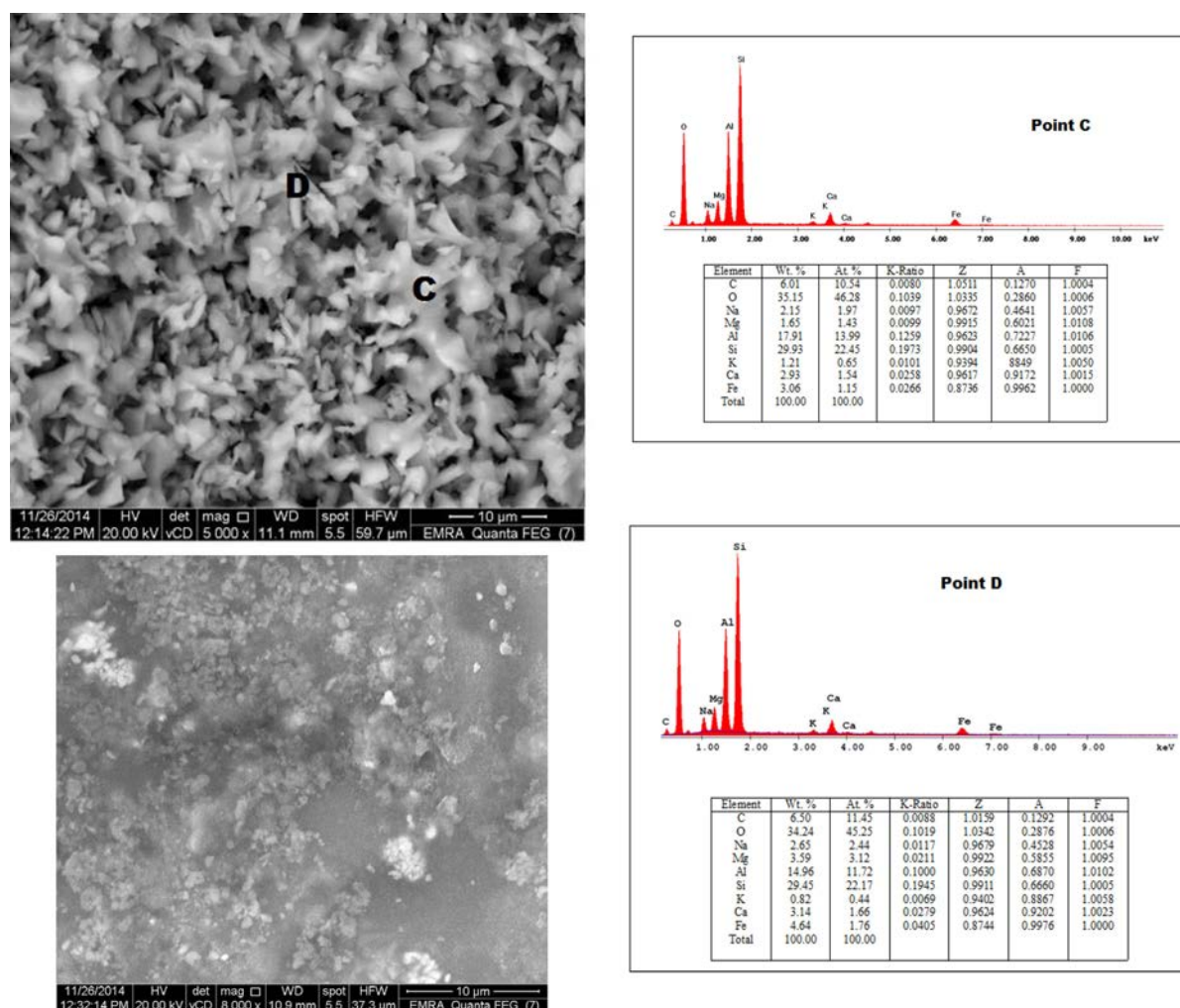


Fig. 13. SEM and EDAX analysis of the selected sample 7 fired at 1150 °C.

liquid phase together with mullite crystals (Points C and D). EDAX results confirm the previous prediction i.e. point A is composed mainly of oxygen (50.15 %) and silicon (48.87%) confirming the presence of quartz crystals, while points B, C and D containing considerable contents of aluminum (12.23, 17.91 and 14.96%) in addition to oxygen (41.84, 35.15 and 34.24%) and silicon (44.04, 29.93 and 29.45%), respectively which confirm the presence of mullite mineral together with quartz. The presence of low quantities of sodium, potassium, calcium and iron together with aluminum, silicon and oxygen confirm the presence of glassy phases. Some residual peaks of carbon appear resulting from coating the samples with graphite during their processing for testing with SEM, so they should be disregarded. This good assemblage of minerals (mullite-quartz dissolved in the glassy phases) explain the improved texture and hence densification and mechanical properties of such samples. The relatively higher contents of impurities in sample 7 (points C and D) than sample 3 (points A and B) drastically affect the mullitization process [24] which explain the relatively better densification and

mechanical properties of sample 3 (ceramic bodies prepared from Ghola albite) than sample 7 (containing Ofsan albite).

Conclusions

From the above results the following conclusions could be remarked;

- According to the ISO 13006 standard, a mixture of 50 wt.% clay, 40 wt.% albite and 10 wt.% quartz (samples 3 and 7) was selected as representative composition of vitreous ceramic tiles and can be classified as group I (water absorption < 3%) and also sub-classified as group BIb (vitrified ceramic tiles, 0.5% < water absorption < 3%).
- The fired samples are homogeneous and have a compact microstructure with absence of cracks, holes, bubbles and pores.
- Higher amount of fluxes (> 40 wt.%, samples 4 and 8) above the vitrification range has a negative effect on physical properties of the ceramic body due to expulsion of the entrapped gases.

- XRD of the fired samples shows that they composed mainly of quartz, mullite and albite minerals. The content of the formed mullite is correlated with the clay content in the ceramic batch.
- SEM and EDX analysis confirm the formation of mullite with quartz dispersed in the glassy phase leading to an improvement in sintering and mechanical properties of the prepared ceramic bodies.

References

1. D. Tavakolia, A. Heidari and M. Karimian, *Asian J. Civ. Eng.* 14[5] (2013) 369-382.
2. N.M. Khalil, *J. Ind. Eng. Chem.* 20[5] (2014) 3663-3666.
3. P. Corma, "Innovations and innovative processes in the Castellón ceramic district" (Qualicer, 2008) P.BA 59-78.
4. G. Nasseti, *Mater. Sci. Eng. A109* (1989) 417- 425.
5. G.A. Khater, *J. Non. Cryst. Solids* 54 (2010) 3066-3070.
6. D. Njoya, M. Hajjaji, A. Baçaoui and D. Njopwouo, *Mater. Charac.* 61 (2010) 289-295.
7. W.E. Lee, G.P. Souza, C.J. McConville and T. Tarvornpanich and Y. Iqbal, *J. Eur. Ceram. Soc.* 28 (2008) 465-471.
8. D.J. Agenor, H. Dachamir, C.S. Vicente, S.V. Enrique, *Mater. Sci. Eng. A725* (2010) 1730-1735.
9. M. Jorge, R. Jesús, R. Maximina, *J. Eur. Ceram. Soc.* 30 (2010) 1599-1607.
10. D.U. Tulyaganov, S. Agathopoulos, H.R. Fernandes and J.M.F. Ferreira, *J. Eur. Ceram. Soc.* 26 (2006) 1131-1139.
11. C. Guyot, in "Comportement d'une pâte céramique vitreuse en cuisson accélérée: influence des différents constituants et de leurs propriétés" (Université d'Orleans, 1997) p. 167.
12. G. Stathis, A. Ekonomakou, C.J. Stournaras and C. Ftikos, *J. Eur. Ceram. Soc.* 24 (2004) 2357-2366.
13. S.R. Bragança and C.P. Bergmann, *J. Eur. Ceram. Soc.* 24 (2004) 2383-2388.
14. K. Schindler, A. Roosen, T. Jüttner and G. Rösler, *J. Eur. Ceram. Soc.* 27 (2007) 1889-1892.
15. L.S. Correia, G. Dienstmann, V.M. Folguerasa and A.M. Segadaes, *J. Hazardous Mater.* 163 (2009) 315-322.
16. T.K. Mukhopadhyay, S. Ghatak and H.S. Maiti, *Ceram. Int.* 35 (2009) 1493-1500.
17. T. Tarvornpanich, G.P. Souza and W.E. Lee, *J. Am. Ceram. Soc.* 91[7] (2008) 2264-2271.
18. T. Tarvornpanich, G.P. Souza and W.E. Lee, *J. Am. Ceram. Soc.* 91[7] (2008) 2272-2280.
19. J. Martýn-Marquez, J.M. Rincon and M. Romero, *Ceram. Int.* 34 (2008) 1867-1873.
20. G.P. Souza, E. Rambaldi, A. Tucci, L. Esposito and W.E. Lee, *J. Am. Ceram. Soc.* 87[10] (2004) 1959-1966.
21. S.M. Naga, F. Bondioli, M.M.S. Wahsh and M. El-Omla, *Ceram. Inter.* 38 (2012) 6267-6272.
22. W.D. Kingery, in "Introduction to Ceramics" (J. Wiley & Sons, 1976)
23. J. Martýn-Marquez, J.M. Rincon, M. Romero, *J. Eur. Ceram. Soc.* 30 (2010) 3063-3069.
24. M.F. Zawrah and N.M. Khalil, *Ceram. Inter.* 27 (2001) 689-694.